Director configuration of planar solitons in nematic liquid crystals

Henryk Arodź and Joachim Stelzer
Instytut Fizyki, Uniwersytet Jagielloński, Reymonta 4, 30-059 Kraków, Poland
(Received 16 September 1997)

The director configuration of disclination lines in nematic liquid crystals in the presence of an external magnetic field is evaluated. Our method is a combination of a polynomial expansion for the director and of further analytical approximations which are tested against a numerical shooting method. The results are particularly simple when the elastic constants are equal, but we discuss the general case of elastic anisotropy. The director field is continuous everywhere apart from a straight line segment whose length depends on the value of the magnetic field. This indicates the possibility of an elongated defect core for disclination lines in nematics due to an external magnetic field. [S1063-651X(98)15602-7]

PACS number(s): 61.30.Jf, 11.27.+d

I. INTRODUCTION

Nematic liquid crystals are systems which are positionally disordered, but reveal a long-range orientational order [1]. This property is described on a mesoscopic level by a unit vector field $\boldsymbol{n}(\boldsymbol{r})$, which is called *director*. Due to the absence of a permanent polarization in the nematic phase the director just indicates the orientation, but its has neither head nor tail. This particular feature yields very interesting defect structures in nematic liquid crystals. For instance, the director field shows line defects in three dimensions (or, equivalently, point defects in two dimensions), called *disclinations*, which have been studied and classified by topological methods [2–5]. Unlike in spin systems, disclinations of topological charge $\pm\frac{1}{2}$ are possible and stable in nematics. When an external magnetic field is applied perpendicular to such a disclination line, the resulting director configuration becomes even more interesting; it can be regarded as a domain wall filling a half-plane which terminates in the disclination line. Such walls with edges, known as planar solitons [6], have been discussed for superfluid ^{3}He by Mineyev and Volovik [7]. Whereas the qualitative behavior of these solitonlike objects is well-established, a quantitative understanding of their structure can be obtained only from a thorough analysis of the underlying field theory. Its is the aim of our paper to perform such calculations. Our approach is based on a polynomial expansion of the director field. This method has been used previously both in relativistic field theories [8,9] and for the evaluation of domain wall dynamics in nematics [10]. It yields approximate analytical solutions for the director orientation.

The paper is organized as follows. In Sec. II the director field equation for the planar solitons is derived. Section III develops a method for obtaining an approximate solution for the tilt angle of the director. Our technique is a combination of the polynomial expansion [8–10] with further approximations that are tested by means of a numerical shooting method [11]. The discussion is performed within the framework of the Oseen-Zöcher-Frank elasticity [12–14]. In Sec. IV we estimate the energy of the defect core of the planar solitons, and we minimize the total energy of the solitons in order to determine the length of the core. Section V contains concluding remarks.

II. DIRECTOR FIELD EQUATION AND BOUNDARY CONDITIONS FOR PLANAR SOLITONS

A. Free energy and field equation

The geometry for planar solitons in nematic liquid crystals is drawn schematically in Figs. 1 (positive soliton) and 2 (negative soliton). The director field is essentially planar, perpendicular to a disclination line of strength $\pm\frac{1}{2}$ along the z direction of a Cartesian coordinate frame. Because the structure is independent on z, we restrict ourselves to the x-y plane ($z=0$). Now we impose a magnetic field in the plane of the director along the x axis. Due to the magnetic anisotropy of the nematic the director tends to align along the magnetic field. However, the topological charge of the disclination has to be conserved. The resulting structure is a planar domain wall of Néel type [15,16,10], which ends in the disclination line [7,6]. Locally, close to the disclination, the director field preserves the defect structure. However, in a plane at a finite distance from the disclination line, which is given by the half width y_0 of the planar Néel wall (Figs. 1 and 2), the director field is aligned parallel to the external magnetic field [7,6].

Due to the translational symmetry along the z axis it is sufficient to perform the calculations in two dimensions only.

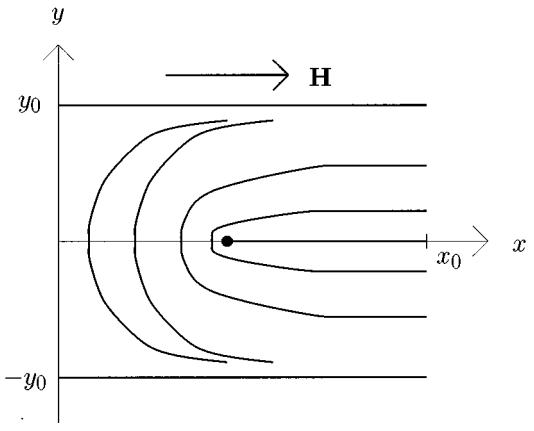

FIG. 1. Geometry and coordinates for a positive planar soliton in a nematic liquid crystal.

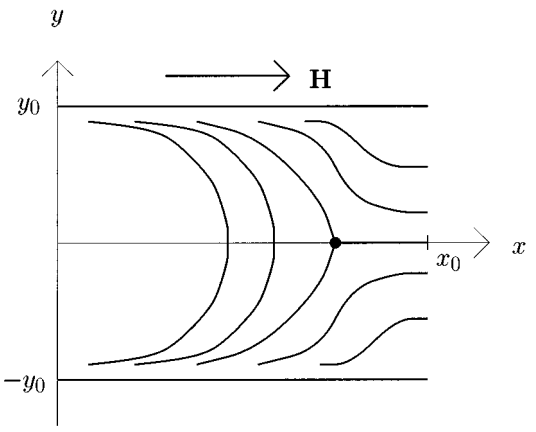

FIG. 2. Geometry and coordinates for a negative planar soliton in a nematic liquid crystal.

The director orientation is then completely determined by the *tilt angle field* $\Phi(x,y)$, which is measured with respect to the direction of the magnetic field $\boldsymbol{H}$ (x axis),

$$\boldsymbol{n}=\cos\Phi(x,y)\hat{\boldsymbol{x}}+\sin\Phi(x,y)\hat{\boldsymbol{y}}, \quad \boldsymbol{H}=H_0\hat{\boldsymbol{x}}. \tag{1}$$

We look for static director configurations, hence Φ does not depend on time.

The geometry of Figs. 1 and 2 holds for nematic materials with positive magnetic anisotropy $\Delta\chi$. The same director configuration can be achieved for negative $\Delta\chi$, too. In the latter case the magnetic field should be applied along the y direction.

The static director orientation inside the soliton corresponds to a configuration minimizing the total free energy F (per unit length in the z direction) which contains both the energy of the nematic phase $F_{\rm nem}$ and the core energy of the disclination $F_{\rm core}$. (Within the defect core local phase transitions may occur.) The nematic energy $F_{\rm nem}$ is the area integral of a free energy density $\mathcal{F}_{\rm nem}$. This free energy density, in turn, consists of elastic contributions (due to distortions of the director field) and of a magnetic part (taking into account the interaction of the nematic with the external magnetic field), hence $\mathcal{F}_{\rm nem}=\mathcal{F}_{\rm elast}+\mathcal{F}_{\rm mag}$. The elastic free energy density follows from the Oseen-Zöcher-Frank expression [12–14],

$$\mathcal{F}_{\rm elast}=\tfrac{1}{2}K_{11}(\text{div }\boldsymbol{n})^2+\tfrac{1}{2}K_{33}(\boldsymbol{n}\times\text{curl }\boldsymbol{n})^2. \tag{2}$$

In Eq. (2) K_{11} and K_{33} denote the elastic constants for *splay* and *bend* deformations in the nematic. Due to the restriction to planar director fields according to Eq. (1) there are no *twist* deformations and the elastic constant K_{22} does not enter the calculations.

The magnetic free energy density couples the director $\boldsymbol{n}$ to the magnetic field $\boldsymbol{H}$ via the anisotropy of the magnetic susceptibility $\Delta\chi$ (μ_0 means the magnetic field constant)

$$\mathcal{F}_{\rm mag}=-\tfrac{1}{2}\mu_0\Delta\chi(\boldsymbol{n}\cdot\boldsymbol{H})^2. \tag{3}$$

When inserting the ansatz for the planar director field (1) into Eqs. (2) and (3), we obtain the free energy density $\mathcal{F}_{\rm nem}$ of the nematic phase,

$$\begin{aligned}\mathcal{F}_{\rm nem}=&\tfrac{1}{4}(K_{11}+K_{33})(\Phi_x^2+\Phi_y^2)+\tfrac{1}{4}(K_{33}-K_{11})(\Phi_x^2-\Phi_y^2)\\&\times\cos2\Phi+\tfrac{1}{2}(K_{33}-K_{11})\Phi_x\Phi_y\,\sin2\Phi\\&-\tfrac{1}{4}\mu_0\Delta\chi H_0^2(1+\cos2\Phi).\end{aligned} \tag{4}$$

In Eq. (4) Φ_x and Φ_y denote partial derivatives of the tilt angle with respect to the spatial coordinates. The energy of the defect core $F_{\rm core}$ will be discussed separately in Sec. IV.

The director configuration for the planar soliton, which minimizes the energy of the nematic phase, follows as a solution of the corresponding Euler-Lagrange equation

$$\frac{\delta\mathcal{F}_{\rm nem}}{\delta n_i}\equiv\frac{\partial\mathcal{F}_{\rm nem}}{\partial n_i}-\partial_j\left(\frac{\partial\mathcal{F}_{\rm nem}}{\partial(\partial_j n_i)}\right)=0. \tag{5}$$

The resulting equation for the tilt angle field $\Phi(x,y)$ can be written in the following form:

$$\begin{aligned}&\Phi_{xx}+\Phi_{yy}+\overline{K}[\partial_x(\Phi_x\cos2\Phi)-\partial_y(\Phi_y\cos2\Phi)]\\&+\overline{K}[\partial_x(\Phi_y\sin2\Phi)+\partial_y(\Phi_x\sin2\Phi)]+\overline{K}(\Phi_x^2-\Phi_y^2\\&-2\Phi_x\Phi_y)\sin2\Phi-\frac{\mu_0\Delta\chi H_0^2}{K_{11}+K_{33}}\sin2\Phi=0,\end{aligned} \tag{6}$$

where

$$\overline{K}=\frac{K_{33}-K_{11}}{K_{11}+K_{33}}$$

is the elastic anisotropy.

B. Boundary conditions

The boundary conditions are an essential feature of the planar solitons. As discussed above, the defect structure is surrounded by a homogeneous director field and by a planar Néel wall. According to the choice of our Cartesian coordinate frame (Figs. 1 and 2) the tilt angle should be zero at $y=\pm y_0$, where y_0 is the half width of the Néel wall. Additionally, it should glue smoothly to the homogeneous orientation. Thus the boundary conditions in the y direction (perpendicular to the magnetic field) are given by

$$\begin{aligned}\Phi(x,y=y_0)&=0,\\ \Phi(x,y=-y_0)&=\pm\pi,\\ \Phi_y(x,y=\pm y_0)&=0,\end{aligned} \tag{7}$$

where $\pm\pi$ is for the positive and negative soliton, respectively.

In the x direction (parallel to the magnetic field), the director field at $x\leqslant0$ coincides with the planar Néel wall. For increasing x coordinate the domain wall structure is destroyed and the director field changes towards the homogeneous orientation, parallel to the magnetic field, which is reached at x_0. Hence,

$$\Phi(x=0,y)=\Phi_{\rm Neel}(y), \quad \Phi(x=x_0,y)=0. \tag{8}$$

It is important to note that the value of x_0 is yet unknown at this stage.

The function $\Phi_{\mathrm{Neel}}(y)$ describes the director inversion due to the planar Néel wall. It can be determined by solving the field equation (6) in one dimension. For $x \leqslant 0$ there is no dependence on the coordinate x and the field equation is simplified to

$$(1-\overline{K}\cos 2\Phi)\Phi_{yy}+\overline{K}\Phi_y^2 \sin 2\Phi-\frac{\mu_0\Delta\chi H_0^2}{K_{11}+K_{33}}\sin 2\Phi=0. \tag{9}$$

The center line of the cross section of the domain wall with the x-y plane coincides with the line $x \leqslant 0$, $y=0$, with tilt angle $\Phi=\pm\pi/2$ on it. Now, following the approach developed in our recent publication [10], we apply a *polynomial expansion* of the tilt angle up to third order in the distance y from the center line,

$$\Phi_{\mathrm{Neel}}(y)=\pm\frac{\pi}{2}\mp\frac{3\pi}{4}\frac{y}{y_0}\pm\frac{\pi}{4}\left(\frac{y}{y_0}\right)^3. \tag{10}$$

The different signs are valid for positive and negative solitons, respectively. Due to the choice of the coefficients in the expansion (10), the boundary conditions (7) are fulfilled. With the approximate expression (10) for $\Phi_{\mathrm{Neel}}(y)$ we can satisfy Eq. (9) up to terms proportional to the first power of y. This fixes the half width y_0 of the planar Néel wall,

$$y_0=\frac{3\pi}{4H_0}\sqrt{\frac{K_{\mathrm{Neel}}}{\mu_0\Delta\chi}},\quad K_{\mathrm{Neel}}=\left(1+\frac{32}{9\pi^2}\right)K_{33}-K_{11}. \tag{11}$$

It is of the order of the magnetic coherence length. Equations (11) and (10) are used in Eq. (8), which now provides the boundary conditions in the x direction.

The approximate solution (10) could be improved by taking a higher order polynomial. If it is of the order y^n, then Eq. (9) can be satisfied up to terms proportional to y^{n-2}. In the present paper we shall restrict ourselves to cubic polynomials in y, which are sufficient to reveal our method of obtaining the approximate director field for the planar soliton.

III. TILT ANGLE FIELD FOR PLANAR SOLITONS

Our strategy for solving the nonlinear partial differential equation (6) for the tilt angle $\Phi(x,y)$ proceeds in two steps. First we apply the polynomial expansion of the tilt angle field in the y coordinate. After separating the y dependence, we are left with a set of ordinary differential equations which is solved both numerically and, approximately, analytically. Of course, the polynomial expansion in y must satisfy the boundary conditions (7). Therefore, up to third order [in congruence with the expansion for the Néel wall (10)] it reads

$$\Phi(x,y)=\left(\pm\frac{\Phi_0(x)}{y_0^2}+C(x)y\right)(y\mp y_0)^2 \mod \pi,$$

$$\text{for}\quad y\geqslant 0,\ y\leqslant 0\quad \text{resp.} \tag{12}$$

The polynomial expansion (12) contains two unknown functions $\Phi_0(x)$ and $C(x)$ that depend on the x coordinate. We can derive boundary conditions for them by inserting Eq. (12) into Eq. (8). This yields (for the positive solitons)

$$\Phi_0(x=0)=\frac{\pi}{2},\quad \Phi_0(x=x_0)=0, \tag{13}$$

$$C(x=0)=\frac{\pi}{4y_0^3},\quad C(x=x_0)=0. \tag{14}$$

Our ansatz (12) is continuous everywhere apart from the x axis ($y=0$). When crossing the x axis between $x=0$ and $x=x_0$, a jump in the director orientation from $+\Phi_0(x)$ to $-\Phi_0(x)$ occurs. This is connected to the physical singularity of the disclination line in the center of the defect. Most significantly, due to the influence of the external magnetic field the cross section of the defect core is no more a pointlike object in the x-y plane, but it is extended to a segment of a straight line of length x_0. However, although the core of the defect is now striplike (if we take into account the z direction), one can define its center line. It is located at $x=x_d$, where $\Phi_0(x=x_d)=\pi/4$, which gives the largest jump (equal to $\pi/2$) in the director orientation at $y=0$. At $x \leqslant 0$ there is no physical singularity, because $\Phi_0=-\pi/2$ is equivalent to $\Phi_0=+\pi/2$.

The discontinuity of Eq. (12) at $y=0$ reflects the fact that the continuum approach is no more valid close to the defect core, where strong gradients of the orientational order are apparent. On a molecular length scale around the core the mesoscopic director loses its physical significance as the average molecular orientation. Remarkably, although when using the director approach we cannot determine the orientational order within the defect core, our investigation gives hints on a possible elongated shape of the core of the disclination line in the presence of the magnetic field. The extension of the defect core (i.e., the actual value of x_0) can only be determined when including the core energy into the investigation. This will be performed in the following section.

We now proceed by inserting the third order polynomial expansion (12) into Eq. (6). By comparison of the coefficients for the first two powers in the y coordinate (i.e., y^0, y^1) we obtain two ordinary differential equations for the unknown expansion coefficients $\Phi_0(x)$ and $C(x)$. It is convenient to change to a set of dimensionless variables by measuring all length scales in units of y_0,

$$x=y_0\overline{x},\quad \Psi=2\Phi_0,\quad \Gamma=y_0^3C. \tag{15}$$

We also introduce the notation

$$\frac{1}{\eta^2}=1+\left(1+\frac{9\pi^2}{16}\right)\overline{K}.$$

The equations for Ψ and Γ have the following form:

$$\tfrac{1}{2}(1+\overline{K}\cos\Psi)\Psi''+(1-\overline{K}\cos\Psi)(\Psi-4\Gamma)-\overline{K}[\tfrac{1}{4}\Psi'^2-(\Gamma-\Psi)^2]\sin\Psi+2\overline{K}(\Gamma'-\Psi')\sin\Psi+2\overline{K}(\Gamma-\Psi)\times\Psi'\cos\Psi-\overline{K}(\Gamma-\Psi)\Psi'\sin\Psi-\frac{1}{\eta^2}\sin\Psi=0 \tag{16}$$

and

$$\tfrac{1}{2}(1+\overline{K}\cos\Psi)(\Gamma''-\Psi'')-\frac{1}{2}\overline{K}(\Gamma-\Psi)\Psi''\sin\Psi+3(1-\overline{K}\cos\Psi)\Gamma+\overline{K}(\Gamma-\Psi)(\Psi-4\Gamma)\sin\Psi$$
$$-\frac{1}{2}\overline{K}[\Psi'(\Gamma'-\Psi')-2(\Gamma-\Psi)(\Psi-4\Gamma)]\sin\Psi+\overline{K}(\Psi'-4\Gamma')\sin\Psi$$
$$-\overline{K}(\Gamma-\Psi)\left[\frac{1}{4}\Psi'^2-(\Gamma-\Psi)^2\right]\cos\Psi+2\overline{K}(\Gamma-\Psi)(\Gamma'-\Psi')\cos\Psi$$
$$-2\overline{K}\Psi'(\Gamma-\Psi)^2\sin\Psi-\overline{K}\Psi'(\Gamma-\Psi)^2\cos\Psi+2\overline{K}\left[(\Gamma-\Psi)(\Gamma'-\Psi')\right.$$
$$\left.+\frac{1}{2}\Psi'(\Psi-4\Gamma)\right]\cos\Psi-\overline{K}\left[(\Gamma-\Psi)(\Gamma'-\Psi')+\frac{1}{2}\Psi'(\Psi-4\Gamma)\right]\sin\Psi$$
$$-\frac{1}{\eta^2}(\Gamma-\Psi)\cos\Psi=0. \tag{17}$$

In Eqs. (16) and (17), $'$ denotes derivatives with respect to the dimensionless variable $\overline{x}$.

The set of ordinary differential equations (16) and (17) becomes much simpler for the one-constant approximation ($\overline{K}=0$). In this particular case the equations above are equivalent to the following ones:

$$\Psi''=8\Gamma-2\Psi+2\sin\Psi, \tag{18}$$

$$\Gamma''=2\Gamma-2\Psi+2(\Gamma-\Psi)\cos\Psi+2\sin\Psi. \tag{19}$$

Nevertheless, we shall analyze the set (16), (17). It turns out that a numerical solution and, if $\overline{K}$ is not too large, also an approximate analytical solution can be obtained.

According to Eqs. (13) and (14) the boundary conditions (for positive solitons) now read (with $\overline{x}_0=x_0/y_0$)

$$\Psi(\overline{x}=0)=\pi,\quad \Psi(\overline{x}=\overline{x}_0)=0, \tag{20}$$

$$\Gamma(\overline{x}=0)=\frac{\pi}{4},\quad \Gamma(\overline{x}=\overline{x}_0)=0. \tag{21}$$

Equations (16), (17), (20), and (21) define a standard two-point boundary value problem. It can be solved numerically, for instance by a *shooting method* [18,19,11]. Satisfying the boundary conditions at $\overline{x}=0$, the ordinary differential equations (16) and (17) are integrated numerically up to $\overline{x}_0$. The integration constants are adapted iteratively in order to minimize the discrepancy between the numerical solution and the boundary conditions at $\overline{x}_0$. For obtaining solutions for $\Psi(\overline{x})$ and $\Gamma(\overline{x})$ we used a computer code from Ref. [11]. Our calculations were performed for parameters corresponding to the liquid crystalline materials *N*-(*p*-methoxybenzylidene)-*p*- buthylaniline (MBBA) and *p*-azoxyanisole (PAA) (see Sec. IV). In these cases the numerical solution almost coincides with the approximate analytical solution presented below.

An approximate analytical solution of Eqs. (16) and (17) can be achieved, which turns out to be quite accurate, as being revealed by a comparison with the numerical solutions. We start from the observation that the free energy density of the defect core, which corresponds to a disordered phase, is much higher than the typical elastic energy of the nematic. Therefore we expect that the core size x_0 is small in comparison with the half-width of the Néel wall y_0, i.e., $\overline{x}_0=x_0/y_0\ll 1$. Furthermore, Ψ and Γ change by a finite amount on the interval $[0,\overline{x}_0]$, namely, by π or $\pi/4$, respectively. Therefore, the derivatives Ψ', Γ' are of the order $\pi/\overline{x}_0$. They are much larger than Ψ and Γ. One cannot *a priori* exclude that also the second-order derivatives are large, of the order $\pi/\overline{x}_0^2$. The approximation consists of keeping in Eqs. (16) and (17) the leading terms only. Then Eq. (16) reduces to

$$(1+\overline{K}\cos\Psi)\Psi''-\frac{1}{2}\overline{K}\Psi'^2\sin\Psi=0, \tag{22}$$

which can immediately be integrated yielding

$$(1+\overline{K}\cos\Psi)^{1/2}\Psi'=\text{const}. \tag{23}$$

In the same approximation Eq. (17) simplifies to

$$(1+\overline{K}\cos\Psi)(\Gamma''-\Psi'')-\overline{K}\Psi'(\Gamma'-\Psi')\sin\Psi-\frac{1}{2}\overline{K}(\Gamma$$
$$-\Psi)\Psi'^2\cos\Psi-\overline{K}(\Gamma-\Psi)\Psi''\sin\Psi=0. \tag{24}$$

In addition to the smallness of $\overline{x}_0$ one can also exploit the fact that the elastic anisotropy $\overline{K}$ can be rather small. For

example, for MBBA its value is 0.11, while for PAA it is 0.36. Moreover, in Eqs. (22) and (24) $\overline{K}$ is multiplied by the sinus or cosinus of Ψ; this effectively diminishes the significance of the terms proportional to $\overline{K}$ even further. Therefore, it is natural to look for solutions of Eqs. (22) and (24) in the form of an expansion into powers of $\overline{K}$. Up to first order in $\overline{K}$ we obtain

$$\Psi=\pi\left(1-\frac{\overline{x}}{\overline{x}_0}\right)-\frac{1}{2}\overline{K}\sin\left[\pi\left(1-\frac{\overline{x}}{\overline{x}_0}\right)\right]+\mathcal{O}(\overline{K}^2), \tag{25}$$

and

$$\Gamma=\frac{\pi}{4}\left(1-\frac{\overline{x}}{\overline{x}_0}\right)-2\overline{K}\sin\left[\pi\left(1-\frac{\overline{x}}{\overline{x}_0}\right)\right]+\frac{3\pi}{8}\overline{K}\left(1-\frac{\overline{x}}{\overline{x}_0}\right)\times\left(1+\cos\left[\pi\left(1-\frac{\overline{x}}{\overline{x}_0}\right)\right]\right)+\mathcal{O}(\overline{K}^2). \tag{26}$$

A comparison with the numerical solutions of Eqs. (22) and (24) shows that the functions in Eqs. (25) and (26) yield very good approximations up to $\overline{K}=0.6$.

IV. LENGTH OF THE DEFECT CORE

Up to this stage, the length of the planar soliton x_0 (or, equivalently, $\overline{x}_0=x_0/y_0$) is unknown. We fix it by minimizing the total free energy, which includes the elastic and magnetic energy of the nematic phase as well as the energy of the defect core.

Let us first calculate the total nematic energy $F_{\rm nem}$ (per unit length along the z axis) for the soliton extending over the rectangle $0\leqslant x\leqslant x_0$, $-y_0\leqslant y\leqslant y_0$, which contains the core of the defect at $y=0$. Outside this rectangle there is the planar Néel wall at $x\leqslant 0$, $-y_0\leqslant y\leqslant y_0$, and the homogeneous director orientation parallel to the external magnetic field along the three remaining sides of the rectangle. Therefore the rectangle contains the total elastic and magnetic energy of the distorted nematic due to the presence of the defect. It is given by the integral

$$F_{\rm nem}=2\int_0^{x_0}dx\int_0^{y_0}dy\;\;\mathcal{F}_{\rm nem}[\Phi(x,y)], \tag{27}$$

where $F_{\rm nem}$ is given by Eq. (4). For the tilt angle $\Phi(x,y)$ we use the approximate solution according to Eqs. (12), (15), (25), and (26). The integrals in Eq. (27) can be calculated by help of a computer algebra system (e.g., MAPLE). The result has the following form:

$$F_{\rm nem}=\frac{1}{2}(K_{11}+K_{33})\left[\frac{0.58}{\overline{x}_0}-0.72\overline{x}_0+\overline{K}\left(\frac{0.19}{\overline{x}_0}+0.93-11.69\overline{x}_0\right)\right]. \tag{28}$$

The terms proportional to $1/\overline{x}_0$ stem from elastic energy terms in $\mathcal{F}_{\rm nem}$ proportional to Φ_x^2. Due to these terms the elastic energy of a defect with a pointlike core would be infinite, because for such a defect $\overline{x}_0=0$.

The expression (28) would suggest that $\overline{x}_0$ should be as large as possible; then, $F_{\rm nem}$ would be minimal. In fact, this is *not* the case, due to the very large free energy stored in the defect core, where local transitions into disordered phases may occur. Let us perform an estimate of this core energy. (Again, it is understood that we consider the energy per unit length along the z axis.) The energy of the core is due to large gradients in the orientational order, which appear on a *molecular* length scale. Therefore, it cannot be expressed in terms of the mesoscopic director field, but it is related to the molecular interaction potential across the discontinuity in the tilt angle on the segment $0\leqslant x\leqslant x_0$ of the x axis. This molecular interaction energy is small at the beginning and at the end of the core where the molecules on both sides of the segment are almost parallel. However, inside the core the molecules can even be perpendicular to each other. In this latter case the discontinuity of the tilt angle is equal to $\pi/2$, and the separation of centers of mass of the molecules is of the order $\sigma_0/\sqrt{2}$ where σ_0 denotes the molecular length. In the present paper we shall be satisfied with a rough estimate obtained by assuming that the core energy density is given by Eq. (4), when all terms are neglected except for $\frac{1}{4}(K_{11}+K_{33})\Phi_y^2$, with $\Phi_y\approx(\pi/2)/(\sigma_0/\sqrt{2})$. The width of the core is taken to be of the order $\sigma_0/\sqrt{2}$. This yields an estimate for the total energy of the core

$$F_{\rm core}\approx\frac{1}{4}(K_{11}+K_{33})\Phi_y^2x_0\frac{\sigma_0}{\sqrt{2}}=\frac{\pi^2}{8\sqrt{2}}(K_{11}+K_{33})\frac{y_0}{\sigma_0}\overline{x}_0. \tag{29}$$

The total energy of the planar soliton is then $F=F_{\rm nem}+F_{\rm core}$. We now insert Eqs. (28) and (29) and then minimize F with respect to the reduced core length $\overline{x}_0$. It is easy to find out that the $\overline{x}_0$ corresponding to the minimum total energy is given by

$$\overline{x}_0^2=\frac{0.58+0.19\overline{K}}{1.74y_0/\sigma_0-0.72-11.69\overline{K}}. \tag{30}$$

Let us compute $\overline{x}_0$ for particular nematic materials. For *N*-(*p*-methoxybenzylidene)-*p*-buthylaniline (MBBA) at 25 °C [17] the elastic constants are $K_{11}=6.0\times10^{-12}$ N and $K_{33}=7.5\times10^{-12}$ N. The magnetic anisotropy is $\mu_0\Delta\chi=9.7\times10^{-8}$ V s/A m, the molecular length $\sigma_0=30$ Å. The magnetic field strength H_0 is chosen 500 Oe, according to a magnetic flux density $B_0\equiv\mu_0H_0=0.05$ T. Then, the elastic anisotropy is $\overline{K}=0.11$. Equation (11) yields $y_0=3900$ Å. Finally, $\overline{x}_0^2\approx0.0027$, and $x_0\approx202$ Å.

For *p*-azoxyanisole (PAA) at 125°C [17] the elastic constants are $K_{11}=4.5\times10^{-12}$ N and $K_{33}=9.5\times10^{-12}$ N. The magnetic anisotropy is $\mu_0\Delta\chi=12.1\times10^{-8}$ V s/A m, the molecular length $\sigma_0=20$ Å. The magnetic field strength H_0 is again chosen 500 Oe. The elastic anisotropy is $\overline{K}=0.36$, $y_0=4940$ Å, and finally $\overline{x}_0^2\approx0.0015$, $x_0\approx191$ Å.

We notice that in both examples $\overline{x}_0^2$ is rather small, indeed. This is consistent with the assumption leading to the

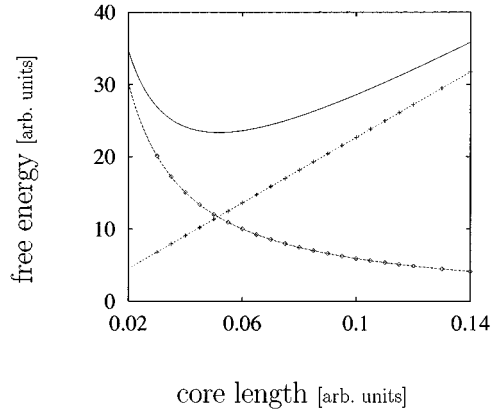

FIG. 3. Free energy (per unit length) F' vs core length $\overline{x_0}$ for MBBA at 25 °C. Both quantities are in arbitrary units (dimensionless). $F'=F/K_{\mathrm{av}}$, $\overline{x_0}=x_0/y_0$, with units $K_{\mathrm{av}}\equiv\frac{1}{2}(K_{11}+K_{33})=6.75\times10^{-12}$ N, $y_0=3900$ Å. Dashed line, analytical solution for the energy of the nematic phase; rhombs, numerical solution for the energy of the nematic phase; dotted line, analytical solution for the energy of the defect core; crosses, numerical solution for the energy of the defect core; solid line, total energy.

approximate solutions (25) and (26). The resulting physical length of the core x_0 is relatively large and it probably could be seen in appropriate experiments. The dependence of the nematic, core, and total energies on the reduced length of the defect core is plotted in Figs. 3 (MBBA) and 4 (PAA).

With the determination of the reduced core length $\overline{x_0}$ the calculation of the director field for the planar soliton is completed. The tilt angle field is shown in Figs. 5 (positive soliton) and 6 (negative soliton). The core line at $y=0$ is clearly visible by the jump of the tilt angle. However, this picture is

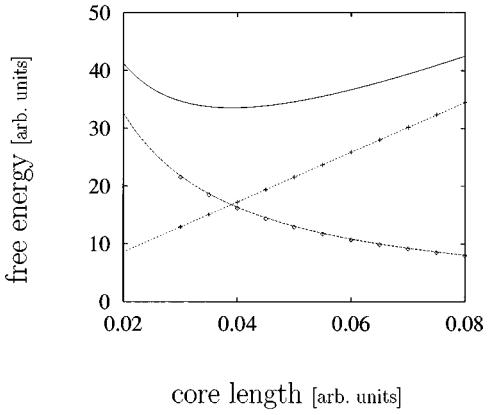

FIG. 4. Free energy (per unit length) F' vs core length $\overline{x_0}$ for PAA at 125 °C. Both quantities are in arbitrary units (dimensionless). $F'=F/K_{\mathrm{av}}$, $\overline{x_0}=x_0/y_0$, with units $K_{\mathrm{av}}\equiv\frac{1}{2}(K_{11}+K_{33})=7\times10^{-12}$ N, $y_0=4940$ Å. Dashed line, analytical solution for the energy of the nematic phase; rhombs, numerical solution for the energy of the nematic phase; dotted line, analytical solution for the energy of the defect core; crosses, numerical solution for the energy of the defect core; solid line, total energy.

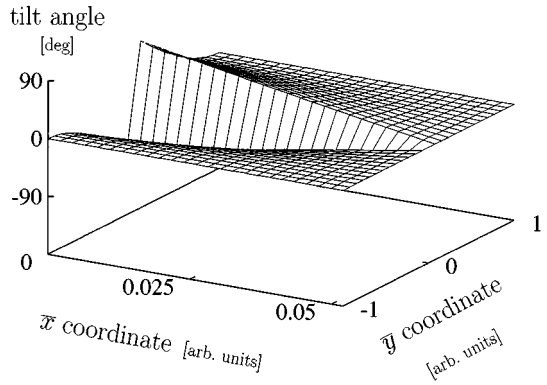

FIG. 5. Tilt angle field for a positive planar soliton in MBBA at 25 °C. Spatial coordinates in arbitrary units. $\overline{x}=x/y_0$, $\overline{y}=y/y_0$ ($y_0=3900$ Å).

somewhat misleading, because it does not take into account that the director is an object without arrowhead. For instance, at $\overline{x}=0$, $\overline{y}=0\pm$ there is a jump by π which in fact means an orientational change of zero angle, exactly the same as for $\overline{x}=\overline{x}_0=0.052$, $\overline{y}=0\pm$. As already stated in the preceding section, due to the periodocity of π for tilt angle changes the largest orientational jump occurs for $\overline{x}_d=0.025$, $\overline{y}_d=0\pm$, where the tilt angle is $\pm\pi/4$. This point can be defined as the center of the core which is related to the original disclination line (in three dimensions).

These particular features become obvious from a lattice visualization of the director field, which is presented in Figs. 7 (positive soliton) and 8 (negative soliton). (In these figures the x and y dimensions are *not* proportionally scaled.) Rods of unitary length placed on the sites of a rectangular lattice indicate the local orientation. The dashed line means the defect core and the small circle marks the center of the core, according to the previous discussion.

V. REMARKS

(i) The positive and negative planar soliton are distinguished by the boundary conditions (20) and (21), but not by

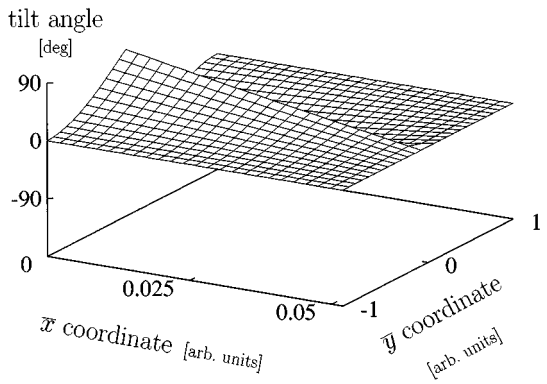

FIG. 6. Tilt angle field for a negative planar soliton in MBBA at 25 °C. Spatial coordinates in arbitrary units. $\overline{x}=x/y_0$, $\overline{y}=y/y_0$ ($y_0=3900$ Å).

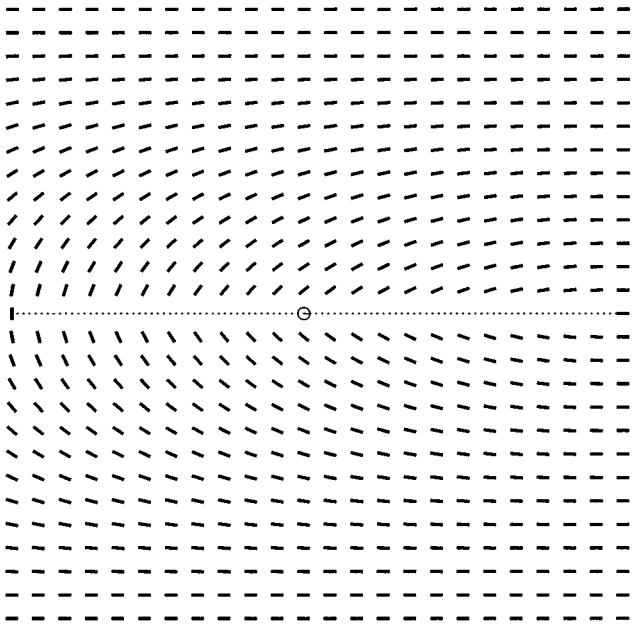

FIG. 7. Lattice visualization of the director configuration for a positive planar soliton.

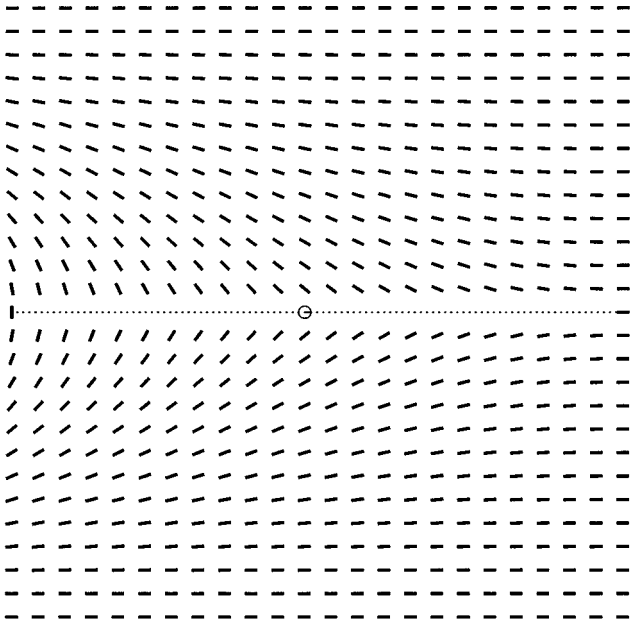

FIG. 8. Lattice visualization of the director configuration for a negative planar soliton.

the field equations. Therefore they cover exactly the same area, although their energy content is slightly different. The tilt angle field for the negative soliton $\Phi^{-}(x,y)$ is obtained from the positive soliton solution $\Phi(x,y)$ presented above by a sign inversion of the expansion coefficients: $\Phi_0^{-}(x) = -\Phi_0(x)$ and $C^{-}(x) = -C(x)$.

(ii) Expression (30) reveals a rather interesting dependence of the reduced core length $\overline{x_0}$ on the magnetic field H_0 which enters through y_0 [see Eq. (11)]. For weak magnetic fields we have large y_0, hence $\overline{x_0}$ is small and it tends to zero when the magnetic field vanishes. However, the physical length of the core is equal to $x_0 = y_0 \overline{x}$ and it increases as $1/\sqrt{H_0}$ when the magnetic field decreases. The physical reason is that for a weaker magnetic field the distance over which the director field can be reorientated by a given angle is larger. In the case of planar solitons the required reorientation is such that the tilt angle changes from $\Phi_{\mathrm{Neel}}(y)$ towards zero. Of course in this limit the width of the Néel domain wall (11) also increases, as $1/H_0$, hence faster. On the other hand, with increasing magnetic field y_0 decreases and $\overline{x_0}$ increases. From inserting Eq. (11) into Eq. (30) it is noticed that formally there is a finite critical value for the magnetic field at which $\overline{x_0}$ becomes infinite. For MBBA the dependence of the reduced and physical core length $\overline{x_0}$ and x_0 on the reduced magnetic field $h \equiv H[\mathrm{Oe}]/500$ is

$$\overline{x_0} = 0.55 \sqrt{\frac{h}{112.8-h}}, \quad \frac{x_0[\text{Å}]}{202} = \frac{10.57}{\sqrt{h(112.8-h)}}, \tag{31}$$

which yields a critical reduced magnetic field $h_c = 112.8$, corresponding to a critical flux density of 5.64 T. However, it should be remembered that Eq. (30) has been derived under the assumption that $\overline{x_0^2}$ is small, so it may become wrong well before reaching the critical value of the magnetic field.

(iii) In the present paper we have assumed that the director configurations in all the planes perpendicular to the z axis are identical. One could attempt an analysis of more general configurations by combining ideas of the present paper and of Refs. [9,10]. In [10] we have evaluated the time evolution of cylindrical Bloch and Néel domain walls in a nematic liquid crystal, and in [9] the dynamics of a generic, curved relativistic domain wall in a scalar field model is investigated; in both papers the polynomial approximation is used. Within a generalized calculation we expect that the functions C and Φ_0 in the polynomial expansion, as well as the half-width y_0 of the Néel wall would depend on the coordinates x, z, and on time t. The variable y would have to be interpreted as a comoving coordinate [9,10]. The director configuration will be time-dependent in general. Equations for C, Φ_0, and y_0 could be obtained from the torque balance [10]

$$\gamma_1 \frac{\partial n_i}{\partial t} + \frac{\delta \mathcal{F}}{\delta n_i} = 0, \tag{32}$$

where γ_1 is the rotational viscosity of the nematic. Because of the larger number of independent variables, such equations will be much more difficult to solve, and we expect that approximate analytical solutions can be found only in some particular cases. On the other hand, one may expect that due to the viscous torques the evolution of the director field $\boldsymbol{n}(\boldsymbol{r},t)$ will terminate in a stable, time-independent configuration of minimum energy. The planar soliton defect discussed in the present paper is probably an example of such a stable configuration.

To conclude, we found an approximate solution for the director configuration in planar solitons in nematics. It is continuous everywhere apart from a strip of finite width. This points out the possibility of an elongated shape of the defect core in disclination lines due to an external magnetic field.

ACKNOWLEDGMENTS

The paper was supported in part by KBN Grant No. 2 P03B 095 13. J.S. gratefully acknowledges his individual grant from the Alexander-von-Humboldt Stiftung.

[1] P. G. de Gennes and J. Prost, *The Physics of Liquid Crystal* (Oxford Science Publications, Clarendon Press, Oxford, 1993).
[2] G. Toulouse and M. Kléman, J. Phys. (France) Lett. **37**, L149 (1976).
[3] N. D. Mermin, Rev. Mod. Phys. **51**, 591 (1979).
[4] V. P. Mineyev, Sov. Sci. Rev. **A 2**, 173 (1980).
[5] H.-R. Trebin, Adv. Phys. **31**, 195 (1982).
[6] S. Chandrasekhar, *Liquid Crystals* (Cambridge University Press, Cambridge, 1992).
[7] V. P. Mineyev and G. E. Volovik, Phys. Rev. B **18**, 3197 (1978).
[8] H. Arodź and A. L. Larsen, Phys. Rev. D **49**, 4154 (1994).
[9] H. Arodź, Phys. Rev. D **52**, 1082 (1995).
[10] J. Stelzer and H. Arodź, Phys. Rev. E **56**, 1784 (1997).
[11] W. T. Vetterling, W. H. Press, S. A. Teukolsky, and B. P. Flannery, *Numerical Recipes* (Cambridge University Press, Cambridge, 1985).
[12] C. W. Oseen, Trans. Faraday Soc. **29**, 883 (1933).
[13] H. Zöcher, Trans. Faraday Soc. **29**, 945 (1933).
[14] F. C. Frank, Discuss. Faraday Soc. **25**, 19 (1958).
[15] L. Néel, J. Phys. Radium **17**, 250 (1956).
[16] W. Helfrich, Phys. Rev. Lett. **21**, 1518 (1968).
[17] M. J. Stephen and J. P. Straley, Rev. Mod. Phys. **46**, 617 (1974).
[18] R. Kippenhan, A. Weigert, and E. Hofmeister, Methods. Comp. Phys. **7**, 129 (1968).
[19] F. S. Acton, *Numerical Methods That Work* (Harper and Row, New York, 1970).